Current Research in Food Science 8 (2024) 100719

Contents lists available at ScienceDirect

Current Research in Food Science

journal homepage: www.sciencedirect.com/journal/current-research-in-food-science

The number and position of unsaturated bonds in aliphatic aldehydes affect meat flavorings system: Insights on initial Maillard reaction stage and meat flavor formation from thiazolidine derivatives

Wenbin Du [a], Yutang Wang [a], Qianli Ma [b], Yang Li [a], Bo Wang [a], Shuang Bai [c], Bei Fan [a,*], Fengzhong Wang [a,**]

[a] Institute of Food Science and Technology, Chinese Academy of Agricultural Sciences, Key Laboratory of Agro-Products Processing, Ministry of Agriculture, Beijing, 100193, China
[b] The First Hospital of Lanzhou University, Lanzhou, 730000, China
[c] Beijing Advanced Innovation Center for Food Nutrition and Human Health, Beijing Technology and Business University, Beijing, 100048, China

ARTICLE INFO

Handling Editor: Dr. Xing Chen

Keywords:
Aliphatic aldehydes
Unsaturated bond
Maillard reaction
Intermediates
Flavor formation

ABSTRACT

Nonanal, (*E*)-2-nonenal, (*E,E*)-2,4-nonadienal, and (*E,Z*)-2,6-nonadienal were used to study the effect of number and position of the unsaturated bond in aliphatic aldehydes on meat flavorings. Cysteine-Amadori and thiazolidine derivatives were synthesized, identified by UPLC-TOF/MS and NMR, and quantitatively by UPLC-MS/MS. The polyunsaturated aldehydes exhibited higher inhibition than monounsaturated aldehydes, and monounsaturated aldehydes exhibited higher inhibition than saturated aldehydes, mainly manifested by the inhibition of the cysteine-Amadori formation and acceleration of the thiazolidine derivatives formation. The effect of unsaturated bonds position in aliphatic aldehydes on the initial Maillard reaction stage was similar. The cysteine played an important role in catalyzing the reaction of aliphatic aldehydes. A total of 109 volatile compounds derived by heating prepared thiazolidine derivatives degradation were detected by GC-MS. Formation pathways of volatile compounds were proposed by retro-aldol, oxidation, etc. Particularly, a route to form thiazole by the decarboxylation reaction of thiazolidine derivatives which derivatives from formaldehyde reacting with cysteine was proposed.

1. Introduction

Controlling flavor is a key factor for the Maillard reaction meat flavorings. Lipid-controlled the Maillard reaction meat flavorings has been extensively studied. Lipid degradation and the Maillard reaction play a key role in the formation of food aroma during meat flavorings processing (Mottram, 1998). In the Maillard reaction, cysteine is known as an important meaty flavor precursor, which could result in the formation of various sulfur-containing compounds. Aliphatic aldehydes come from the oxidative degradation of fatty acids. In the early period, hydroperoxides were formed through the removal of hydrogen free radical for the alkyl radical, the addition of O_2, and absorption of hydrogen free radical (Du et al., 2019; Whitfield, 1992). For example, the degradation of 9- and 10-hydroperoxides of oleic acid and linoleic acid can lead to nonanal, and (*E*)-2-nonenal. It was noteworthy that aliphatic aldehydes not only contribute to fatty flavor, but also change the pathway of Maillard reaction flavors (Wang et al., 2020; Zhao et al., 2019a).

According to the Hodge-scheme, early stage, intermediate stage, and final stage had been investigated by researchers since 1950s. In the early stage, carbonyls of aldoses or ketoses (reducing sugars) react with the amino groups of amino acids by nucleophilic reaction to form a reversible aldosylamines or ketosylamines (Schiff base), which is based on ring opening of the reducing sugar moiety. The aldosylamines/ketosylamines undergo Amadori/Heyns rearrangement reaction to form N-substituted 1-amino-2-deoxyketose/N-substituted 2-amino-1-deoxyaldose named Amadori rearrangement products/Heyns rearrangement products, which were based on the π bond (-C═N-) of the Schiff base which could move towards the reducing sugar moiety. Dried foods were particularly rich in Amadori rearrangement products/Heyns rearrangement products, comprising as much as several percent of the total

* Corresponding author.
** Corresponding author.
E-mail addresses: fanbei517@163.com (B. Fan), wangfengzhong@sina.com (F. Wang).

https://doi.org/10.1016/j.crfs.2024.100719
Received 3 January 2024; Received in revised form 8 March 2024; Accepted 12 March 2024
Available online 12 March 2024

weight (Yu et al., 2018). The general result is that inclusion of lipids and lipid oxidation products in the reaction system of cysteine and reducing sugars tends to reduce the level of sulfur-containing compounds derived solely from the Maillard reaction (Du et al., 2020). Due to the electrophilic properties, it is well established that the reaction of cysteine with aldehydes leads to the formation of thiazolidine-4-carboxylic acids (Yoshitake et al., 2019). On the other hand, when cysteine reacts with an *α,β*-unsaturated aldehyde, the other significant reaction is Michael addition. Briefly, in the interaction between the Maillard reaction and aldehydes, the reducing sugars compete with aliphatic aldehydes to react with cysteine and form nonvolatile intermediates, e.g., 2-threityl-thiazolidine-4-carboxylic acids (TTCA), Amadori compounds, hemiacetals, and thiazolidines (Cui et al., 2018; Fernandez et al., 2001). It was reported that thiazolidine derivatives formed from hexanal, (*E*)-2-heptenal and (*E,E*)-2,4-decadienal reacted with glutathione (Wang et al., 2020). According to our former research, the number and position of unsaturated bonds in aliphatic aldehydes affect the volatile compounds of cysteine-glucose Maillard reaction (Du et al., 2023). However, the effect of aldehydes on changes in the content of Amadori compounds and thiazolidine derivatives have not been reported. Moreover, it has great significance to study the number and position of the unsaturated bond in the aliphatic aldehydes to understand the influence on nonvolatile intermediates formation. For instance, Clark and Deed, (2018) identified 3-S-glutathionylhexanal in grape juices of (*E*)-2-hexenal with GSH (Clark and Deed, 2018). Furthermore, the addition of lipid to the Maillard reaction system inhibits the production of sulfur-containing compounds, resulting in the formation of new alkyl compounds by nucleophilic substitution/addition. It was reported that 2-pentylthiophene was produced from the reaction between (*E,E*)-2, 4-nonadienal and H_2S *via* the Strecker degradation of cysteine (Zhao et al., 2019a). So, it is of great significance to study the compounds' formation pathway and the influence of aliphatic aldehydes on the Maillard reaction.

This study explored the effect of number and position of unsaturated bond in aliphatic aldehydes on initial Maillard reactions meat flavorings in a stew meat model system. It used the essential lipid degradation products of nonanal, (*E*)-2-nonenal, (*E,E*)-2,4-nonadienal and (*E,Z*)-2,6-nondienal, as these key aroma compounds played a significant effect on food flavor (Bi et al., 2019; Li et al., 2023; Pu et al., 2022; Sohail et al., 2022). Intermediates (cysteine-Amadori and thiazolidine derivatives) were synthesized and identified, as standard compounds quantitative in different reaction systems. This study not only compared the reaction degree of the meat flavorings processing, but also predicted the volatile compound formation pathway by thiazolidine derivatives. This objective of the work is helpful to further understand the reaction pathway involving Maillard reaction with the lipid degradation during controlling savory flavoring or meat foods, and can also provide some guidance for efficient preparation of processed-meat flavorings.

2. Materials and methods

2.1. Chemicals

L-Cysteine, D-glucose, nonanal, (*E*)-2-nonenal, (*E,E*)-2,4-nonadienal, (*E,Z*)-2,6-nonadienal, 1,2-dichlorobenzene, and the *n*-alkanes (C_5–C_{30}) were purchasing from J&K Chemical Ltd. (99%, Beijing, China). Dichloromethane, PBS (phosphate buffer, 0.2 M, pH 6.50), Sinopharm Chemical Reagent Co. Ltd. (Shanghai, China). Stand compounds including: 1-hexanethiol (98%), 2-hexylthiophene (98%), 2-propylthiophene (98%), 3,4-dimethylthiophene (98%), 2-butylthiophene (98%), 2-pentylthiophene (98%), 2-pentylfuran (95%), 2-methylpyridine (98%), 5-methyl-2-thiophenecarboxaldehyde (99%), thieno[3,2-b] thiophene (98%), thieno[2,3-b]thiophene (98%), 2-propylthiazole (99%), 2-ethylthiazole (98%), 2-thiophenecarboxaldehyde (98%), and other lipid degradation products (J & K Chemical Co., Ltd. Beijing, China).

2.2. Preparation of the intermediate compounds

Cys-Amadori (*N*-(1-deoxy-D-glucos-1-yl)-L-cysteine) was prepared by L-cysteine (0.02 mol), D-glucose (0.02 mol), was dissolved in 5 mL of PBS, magnetic with stirring in a 15 mL vial, in a water bath, heated at 55 °C for 1 h, and then 85 °C for 6 h, to purify the intermediate product separations were conducted using a preparative column (40 cm × 1.6 cm, Bio-Rad AG 50 W-X 4 (H^+) 200–400 mesh) cation exchange resin, UV monitoring at 220 nm. The reaction mixture had entirely loaded in the column and then eluted gradually with water and 0.15 M ammonia solution, and then was collected and freeze-dried (Hou et al., 2017).

Cys-Amadori: UPLC-TOF/MS (ESI^+) MS: 284.1158 ([M + H] $^+$). Structure 1: ^{1} H NMR (500 MHz, $(CD_3)_2S{=}O$, ppm): *δ* 2.71–2.73 (*d, J* = 8, CH_2-3), 3.03(*s*, CH_2-4), 3.36–3.39(*m*, CH-8), 3.66–3.68 (*m*, CH-6, CH_2-9), 3.69–3.77 (*m*, CH-2, CH-7). ^{13} C NMR (500 MHz, $(CD_3)_2S{=}O$, ppm): *δ* 25.78 (C-3), 59.16 (C-4), 63.99 (C-9), 70.30 (C-2), 65.90 (C-7), 75.02(C-8), 80.23(C-6), 81.03 (C-5), 173.26 (C-1, COO^-). Structure 2: ^{1} H NMR (500 MHz, $(CD_3)_2S{=}O$, ppm): *δ* 2.83–2.84 (*d, J* = 4, CH_2 -3), 3.43–3.47 (*m*, CH-6, CH-7), 3.66–3.68 (*m*, CH-5, CH-8), 3.69–3.77(*d*, CH_2-9), 3.78–3.79(*d, J* = 4, CH-2), 4.72–4.73 (*d, J* = 4, CH-4). ^{13} C NMR (500 MHz, $(CD_3)_2S{=}O$, ppm): *δ* 22.84 (C-3), 63.86 (C-2), 63.65 (C-8), 64.95 (C-7), 72.27 (C-6), 72.34 (C-9), 72.80 (C-5), 72.22 (C-4), 173.09 (C-1, COO^-).

R 1: 2-(octyl)-thiazolidine-4-carboxylic acid; R 2: 2-(1-octenyl)-thiazolidine-4-carboxylic acid; R 3: 2-(1,3-octadienyl)-thiazolidine-4-carboxylic acid; R 4: 2-(1,5-octadienyl)-thiazolidine-4-carboxylic acid. Thiazolidine derivatives were prepared by, i.e., R 1: L-cysteine (2 mmol), nonanal (1 mmol); R 2: L-cysteine (2 mmol), (*E*)-2-nonenal (1 mmol); R 3: L-cysteine (2 mmol), (*E,E*)-2,4-nonadienal (1 mmol); R 4: L-cysteine(2 mmol), (*E,Z*)-2,6-nonadienal (1 mmol). Aliphatic aldehydes were dissolved in 5 mL of ethnaol, cysteine was dissolved in 10 mL of H_2O, magnetic with stirring in a 15 mL glass vial with a screw cap, at room temperature for 12 h. The resulting reaction mixture was separated on a column (40 cm × 1.6 cm, polyamide resin, 125–150 mesh Mitsubishi Chemical Corporation, Tokyo, Japan), UV monitoring: 220 nm. The sample had entirely loaded in the column and then eluted gradually with water and ammonium hydroxide (0.04 M), followed by freeze-dried (Wang et al., 2020).

R 1: UPLC-TOF/MS (ESI^+) MS: 246.1414 ([M + H] $^+$). ^{1} H NMR (500 MHz, $(CD_3)_2S{=}O$, ppm): *δ* 0.84–0.88 (*t, J* = 16 Hz, CH_3-12), 1.17–1.34 (*m*, CH_2-11, CH_2-10, CH_2-9, CH_2-8, CH_2-7, CH_2-6), 1.70–1.77 (*m*, CH_2-5), 2.71–2.77(*d, J* = 24, CH_2-3), 3.67–3.72(*t, J* = 20, CH-4). ^{13} C NMR (500 MHz, $(CD_3)_2S{=}O$, ppm): *δ* 14.42 (C-12), 22.57 (C-11), 29.09 (C-6), 29.34 (C-9), 29.40 (C-8), 31.19 (C-5), 31.75 (C-10), 35.31(C-3), 65.67 (C-4), 71.52 (C-2), 172.78 (C-1, COO^-). R 2: UPLC-TOF/MS (ESI^+) MS: 244.1478 ([M + H] $^+$). ^{1} H NMR (500 MHz, $(CD_3)_2S{=}O$, ppm): *δ* 0.86 (*t, J* = 12 Hz, CH_3-12), 1.27–1.44 (*m*, CH_2-11, CH_2-10, CH_2-9, CH_2-8), 2.05–2.16 (*m*, CH_2-7), 2.86–2.89 (*d, J* = 12 Hz, CH_2-3), 3.39–3.49 (*t, J* = 20 Hz, CH-2), 4.02–4.04 (*d, J* = 8, CH-4), 5.00–5.27 (*m*, CH-5, CH-6). ^{13} C NMR (500 MHz, $(CD_3)_2S{=}O$, ppm): *δ* 14.31 (C-12), 22.37 (C-11), 27.75 (C-9), 29.71 (C-8), 31.28 (C-10), 31.79 (C-7), 33.89 (C-3), 53.03 (C-4), 55.62 (C-2), 122.89 (C-5), 148.54 (C-6), 167.89 (C-1, COO^-). R 3: UPLC-TOF/MS (ESI^+) MS: 242.1313 ([M + H] $^+$). ^{1} H NMR (500 MHz, $(CD_3)_2S{=}O$, ppm): *δ* 0.87 (*t, J* = 12 Hz, CH_3-12), 1.28–1.44 (*m*, CH_2-11, CH_2-10), 2.18–2.22 (*dt, J* = 8 Hz, CH_2-9), 2.76–2.78 (*d, J* = 8 Hz, CH_2-3), 3.37–3.41 (*t, J* = 10 Hz, CH -2), 4.14–4.20 (*d, J* = 24 Hz, CH-4), 5.23–5.31 (*dt, J* = 16 Hz, CH-8), 5.91–6.00 (*dd, J* = 16 Hz, CH-6), 6.33–6.42 (*dd, J* = 8 Hz, CH-7). ^{13} C NMR (500 MHz, $(CD_3)_2S{=}O$, ppm): *δ* 14.20 (C-12), 22.21 (C-11), 29.72 (C-10), 30.64 (C-9), 32.70 (C-3), 55.88 (C-4), 70.89 (C-2), 129.26 (C-5), 130.31 (C-6), 147.63 (C-7), 153.77 (C-8), 194.64 (C-1, COO^-). R 4: UPLC-TOF/MS (ESI^+) MS: 242.1090 ([M + H] $^+$). ^{1} H NMR (500 MHz, $(CD_3)_2S{=}O$, ppm): *δ* 0.91–0.94 (*t, J* = 12 Hz, CH_3-12), 1.98–2.04 (*m*, CH_2-11, CH_2-8, CH_2-7), 2.69–2.71 (*d, J* = 12 Hz, CH_3-3), 3.09–3.12 (*t, J* = 12 Hz, CH-2), 4.45–4.50 (*d, J* = 20 Hz, CH-4), 5.30–5.33 (*m*, CH-10, CH-9), 5.90–5.97 (m, CH-6, CH-5). ^{13} C NMR (500 MHz, $(CD_3)_2S{=}O$, ppm): *δ*

14.57 (C-12), 20.55 (C-11), 25.44(C-7), 32.59 (C-8), 33.92 (C-3), 53.07 (C-4), 55.69 (C-2), 127.86 (C-5), 132.84 (C-6), 133.19 (C-9), 159.36 (C-10), 194.81 (C-1, COO^{-}).

2.3. UPLC-UV analysis

An Acquity UPLC I Class system coupled with a PDA e λ delector (Waters Corporation, Milford, DE, USA) was used. Chromatographic separation was performed by a T 3 column (1.8 μm, 2.1 mm × 100 mm, Waters ACQUITY UPLC HSS T 3, USA). The mobile phase: acetonitrile and ammonium formate (10 mM; 70:30, *v/v*), flowing in isocratic elution mode: 0.25 mL/min. Column oven temperature at 40 °C. The sample injection volume was 2 μL. The product was subjected to UPLC-UV analyses, with purity ≥95%.

2.4. UPLC–Q/TOF qualitative analysis

An Acquity UPLC I Class and Xevo G 2-XS Q Tof system equipped with UPLC and Q/TOF (Waters Corporation, Milford, DE, USA) were used. UPLC conditions were described in the above UPLC-UV analysis, a system equipped with a column T 3 (1.8 μm, 2.1 mm × 10 cm, Waters ACQUITY UPLC HSS T 3, USA). The flowing at 0.25 mL/min. MS ^{E} centroid mode, electrospray ionization (ESI) positive mode. The ion source capillary was 3.0 kV. Sample cone 40 v. The capillary temperature was 150 °C. The collision energy 4 v and Ramp collision energy 10 v. The flow rates of the cone gas and desolvation gas: 50 L/Hr and 900 L/Hr, respectively. The full scan range of mass spectra was set over m/z 40–1200 for MS/TOF detection.

2.5. NMR qualitative analysis

The 20 mg product was used with $(CD_3)_2S{=}O$ as the solvent. ^{1}H NMR and ^{13}C NMR analyses, an AV 500 NMR spectrometer (Bruker, Switzerland).

2.6. UPLC-MS/MS quantitative analysis

An Acquity UPLC H Class PLUS and Xevo TQ - XS system equipped with UPLC and Q/Q/Q (Waters Corporation, Milford, DE, USA) were used. UPLC conditions used were identical to those described in the above UPLC-UV analysis, flowing at 0.25 mL/min. MRM mode and experiment condition are shown in Table S1. Electrospray ionization: ESI, positive ion mode. The ion source capillary was 2.5 kV. Cone was 21 v. The capillary temperature was 250 °C. Flow rates of the cone gas and desolvation gas were 600 L/Hr and 150 L/Hr. Data were acquired with the Xcalibur software system.

2.7. Volatile compounds from the degradation of the intermediates

R 1, R 2, R 3, and R 4 (2 mmol) each were dissolved in 3 mL of PBS (0.2 M, pH 6.50) in a 15 mL pressure vial. The four intermediates model systems were magnetic stirred at 140 °C in an oil bath for 120 min.

SPME (Solid-phase micro-extraction, 50/35 μm Carboxen/polydimethylsiloxane/divinylbenzene fiber, CAR/PDMS/DVB, Supelco Inc., Bellefonte, PA), 1 μL of 1,2-dichlorobenzene solution (internal standard, 100 μg/mL of methanol) was added to intermediates model system containing 3 mL. The pressure vial was equilibrated at 60 °C, for 30 min. The fiber was exposed in the headspace of the pressure vial at 60 °C, for 20 min before GC-MS-O and GC-MS for further analysis.

Gas chromatography-mass spectrometry (GC-MS) and gas chromatography-mass spectrometry-olfactometry (GC-MS-O) analysis. The 7890 B gas chromatograph-5977 A mass spectrometer (Agilent echnology, Santa Clara, CA). The DB-Wax capillary column (30 m × 0.25 mm × 0.25 μm) was used for the flavor compounds, with carrier gas (Helium, 99.999 %) at 1 mL/min. The gas chromatography condition was adjusted with an oven temperature of 40 °C, raised to 205 °C at 3.5 °C/min; and finally raised to 245 °C at 8 °C/min, and the fiber was desorbed for 3.5 min at 230 °C (splitless mode).

The mass detector and the olfactometer (Sniffer 9000, Brechbühler, Schlieren, Switzerland) running model was performed using the method of the literature which we had published before (Du et al., 2023).

2.8. Identification of volatile compounds

The volatile compounds was identified by searching NIST 15 mass spectra library (MS), retention indices (RI, relative to n-alkanes (C_5-C_{30}) in both GC-MS and GC-MS-O analyses), authentic chemicals (S) and odor characteristics (O).

2.9. Statistical analysis

All statistical analyses were the averages of three replicates. The pathways of the volatile compounds were plotted with ChemDraw 7.0, and Origin 2019 b.

3. Results and discussion

3.1. Quantitation of non-volatile components in the system

UPLC-MS/MS (TQXS) is a specialized non-volatile compound quantitative means with high performance. Based on our previous study, to study the influence of the number and position of the unsaturated bond in aliphatic aldehydes on the Maillard reaction system of "cysteine-glucose", the conditions of the meat flavorings system were designed (Du et al., 2019).

As described above, a preliminary reaction scheme was presented for the intermediates formation of cysteine, glucose, and aliphatic aldehydes (nonanal, (*E*)-2-nonenal, (*E,E*)-2,4-nonadienal, and (*E,Z*)-2,6-nonadienal). The protonated carbonyl group of aliphatic aldehydes had strong electrophilicity under acidic conditions, and was prone to nucleophilic addition reaction with amino group of cysteine. After dehydration, imidonium salt were formed. The lone pair electrons on sulfhydryl sulfur attacked the carbon of imminium salts, the π bond break and the electrons transferred, and deprotonated after cyclic closure, forming thiazolidane derivatives. As shown in Fig. 1 (1), thiazolidine derivatives prepared by aliphatic aldehydes reacted with cysteine. In addition, the complex reaction not only leads to the formation of thiazolidine derivatives, which was the aforementioned classical carbonyl addition, but also to the Michael addition of sulfhydryl to the conjugated C═C double bond of *α,β*-unsaturated aldehydes (1,4-conjugate addition) (Adams et al., 2011; Yoshitake et al., 2019). Overall, we were interested in the quantification of nucleophilic addition products of thiazolidine derivatives. Additionally, Fig. 1 (2) was presented, the scheme for the reaction of cysteine and glucose to form cysteine-Amadori intermediate compounds.

The resulting reaction mixture was analyzed by UPLC-MS/MS, Fig. 2 showed the concentrations of nonvolatile compounds of cysteine-Amadori and thiazolidine derivatives compounds in the five reaction mixture system (system M (cysteine-glucose), system A (cysteine-glucose-nonanal), system B (cysteine-glucose-(*E*)-2-nonenal), system C (cysteine-glucose-(*E,E*)-2,4-nonadienal), system D (cysteine-glucose-(*E,Z*)-2,6-nonadienal)). The change in nonvolatile component content can be studied and compared to the reaction degree. As shown in Fig. 2 (thiazolidine derivatives), concentrations of all the intermediates first rose and then fell with reaction time. Although few reaction products were formed resulting from the condensation of cysteine with aldehydes, the cysteine plays an important role in catalyzing the further reaction of these aliphatic aldehydes, especially unsaturated aldehydes (Adams et al., 2011). Regarding thiazolidine derivatives, the maximum concentration occurred first in systems C and D, then system B, and finally system A. System C and D was the first to reach the maximum concentration. The unsaturated aldehydes (*E,E*)-2,4-nonadienal and (*E,*

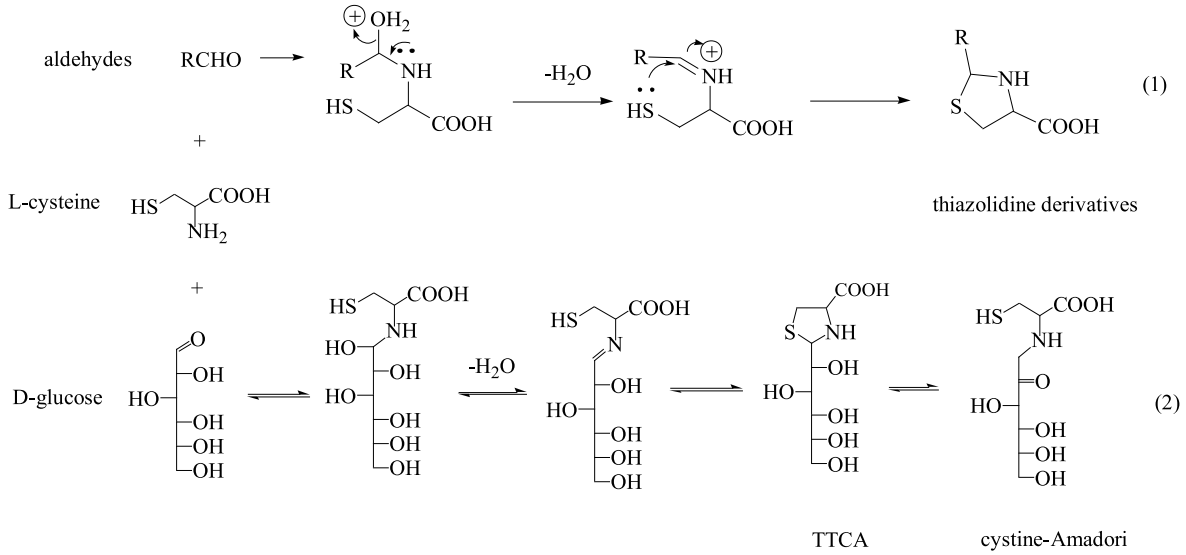

Fig. 1. According to the initial reaction stage, the two major pathways to develop thiazolidine derivatives (1) and Amadori compound (2) in reaction systems.

Z)-2,6-nonadienal exhibited high reactivity against glucose for cysteine, yielding higher levels of thiazolidine derivatives than nonanal and (*E*)-2-nonenal. This phenomenon suggested an acceleration effect of unsaturated bond on rate of the reaction in cysteine-aliphatic aldehydes. Briefly, an amino acid can facilitate the cyclization process by acid catalysis. The zwitterionic form of the amino acid protonates the carbonyl group of the aliphatic aldehydes, thus increasing its electrophilicity, while at the same time the hydroxyl function was deprotonated, increasing its nucleophilicity. This was particularly evident in unsaturated aldehydes. However, the positions of the unsaturated bonds in aliphatic aldehydes in the cysteine-aliphatic aldehydes reaction degree were similar.

The concentration of intermediate compounds in the reaction mixture of the five systems was determined (as shown in Fig. 2 cysteine-Amadori). At 10 min, system M had the highest cysteine-Amadori content, followed by system A, system B, and system C and D, indicating that aliphatic aldehydes inhibited cysteine-Amadori formation, (*E,E*)-2,4-nonadienal and (*E,Z*)-2,6-nonadienal inhibited most markedly. The double bond content in aliphatic aldehydes contributes highly to reaction activity, mainly manifested in inhibition of the initial Maillard reaction and participation in the initial Maillard reaction. These suggested that polyunsaturated aldehydes exhibited higher inhibition on the initial Maillard reaction than monounsaturated aldehydes, monounsaturated aldehydes exhibited higher inhibition on the initial Maillard reaction than saturated aldehydes, because of higher reactivity of the unsaturated aldehydes to react with cysteine against glucose. Other relative differences between the aliphatic aldehydes detected would probably depend on their steric effects.

The concentrations of cysteine-Amadori decreased with reaction time, this was evidenced by their degradation, as obviously seen from Fig. 2. Meanwhile, this dramatic drop suggested that a high rate of amino-carbonyl reaction depleting the amino groups of cysteine occurred at that time, since in the initial reaction period the reactants all had a high concentration. Formation of the cysteine-Amadori component in four systems showed inhibition by the aliphatic aldehydes (nonanal, (*E*)-2-nonenal, (*E,E*)-2,4-nonadienal, and (*E,Z*)-2,6-nonadienal) on cysteine with glucose reaction. Otherwise, according to previous research, the lipid inhibits the Maillard reaction (Yang et al., 2015).

3.2. Structure identification by UPLC-Q/TOF

UPLC-Q/TOF is a high-resolution mass spectrometer especially used for the characterization of compounds because of its high precision and structural elucidation process. According to the chemical structures of the intermediates shown in Fig. 3, cys-Amadori and thiazolidine derivatives were identified by the reaction of aliphatic aldehydes and glucose with cysteine.

As shown in Fig. 3 (cysteine-Amadori), the ions m/z 284.1158 for cysteine-Amadori ($[M + H]^+$), and m/z 248 for cysteine-Amadori with loss of H_2O or 2 H_2O from the carbohydrate moiety of the respective $[M + H]^+$ were revealed with a strong peak. Besides, as shown in Fig. 3 R 1, R 2, R 3, and R 4 (ion m/z 246.1414, 244.1478, 242.1313, 242.1090) due to scission in the carbohydrate chain of the $[M + H]^+$ ion all had a good abundance, indicating thiazolidine derivatives be caught in collision-induced dissociation (CID) during MS/TOF analysis. Moreover, the ions m/z 126 for R 1, m/z 124 for R 2, m/z 122 for R 3, and m/z 122 for R 4 could all be acquired by removal of the alkyl chain from the respective $[M + H]^+$ ion (shown in Fig. 3). The ion m/z 139 for R 2, m/z 169 for R 3, and m/z 169 for R 4 could be acquired by cleavage of the thiazolidine from the respective $[M + H]^+$ ion (shown in Fig. 3).

3.3. Structure identification by NMR

Preparation of cysteine-Amadori and thiazolidine derivatives was performed by isolating the reaction mixture to further elucidate the structures of the intermediates detected by NMR.

The processed NMR data were presented in the previous Section, while the NMR spectra are shown in Fig. S1. As expected, with regards to thiazolidine derivatives (R 1), chemical shifts (ppm) of δ_C 65.67(C-4), δ_C 35.31 (C-3), and δ_C 71.52 (C-2) corresponding to the thiazolidine ring were consistent with the literature (Fernandez et al., 2001; Wang et al., 2020). With regards to R 2 thiazolidine derivatives, the chemical shifts (ppm) of δ_C 122.89 (C-5) and δ_C 148.54 (C-6) corresponded to an olefinic bond. R 3 thiazolidine derivatives, the chemical shifts (ppm) of δ_C 129.26/δ_H 6.00 (C-5), δ_C 130.31/δ_H 5.91 (C-6), δ_C 147.63/δ_H 6.33 (C-7), and δ_C 153.77/δ_H 5.23 (C-8) corresponded to an olefinic bond. Moreover, chemical shifts (ppm) of δ_C 194.64 (C-1), correspond to carboxylic acid. R 4 thiazolidine derivatives, the chemical shifts (ppm) of δ_C 127.86/δ_H 5.97 (C-5), δ_C 132.84/δ_H 5.90 (C-6), δ_C 133.19/δ_H 5.30 (C-9), and δ_C 159.36/δ_H 5.33 (C-10) corresponded to an olefinic bond. The chemical shifts in thiazolidine derivatives compounds showed similar reported results (Wang et al., 2020; Fernandez et al., 2001). However, signals of impurities or environmental contaminants were detected, not labeled with chemical shifts.

The structures of ARP were further confirmed by NMR. It was worth

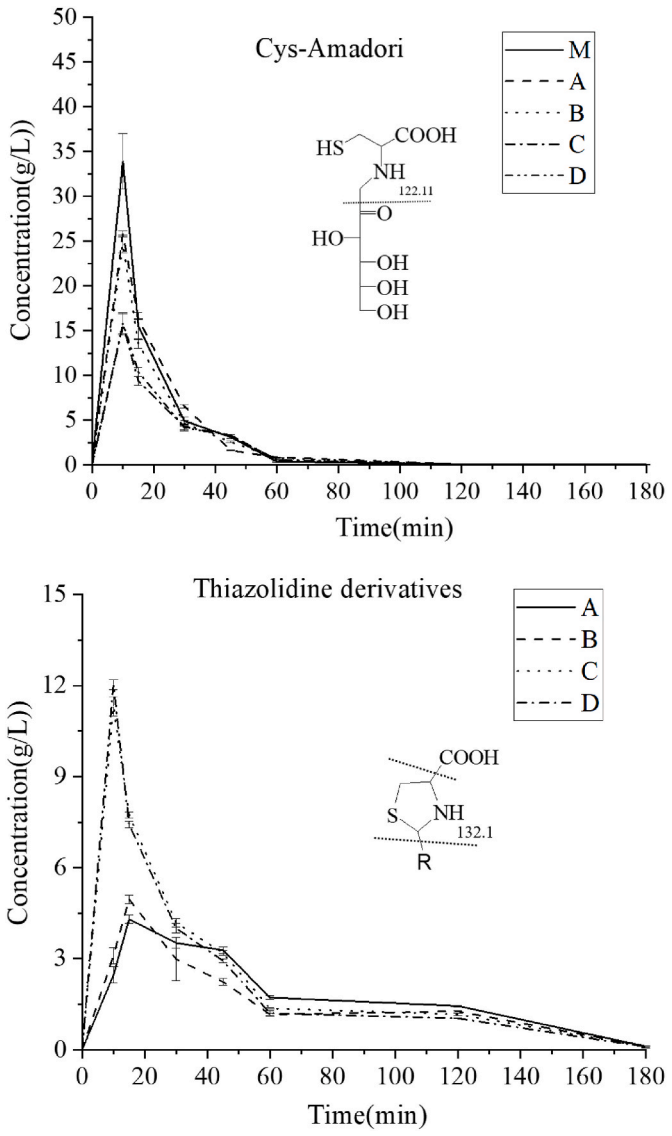

Fig. 2. Concentrations of the detected Amadori compound and thiazolidine derivatives with reaction time in the reaction mixtures (system M (cysteine-glucose), system A (cysteine-glucose-nonanal), system B (cysteine-glucose-(*E*)-2-nonenal), system C (cysteine-glucose-(*E,E*)-2,4-nonadienal), system D (cysteine-glucose-(*E,Z*)-2,6-nonadienal)).

noting that the ARP was not found in the NMR data like the reference (Cao et al., 2017; Hou et al., 2017). The isomers contained were detected in ARP compounds. As expected, the six-membered rings in the structures of isomers. The NMR data presented in Fig. S1 showed that structure 1 and structure 2 signals were in the expected chemical shifts and agreed with those reported in the literature. Regarding structure 1, signals (ppm) of δ_C 25.78/δ_H 2.71 (C-3), δ_C 59.16/δ_H 3.03 (C-4), δ_C 63.99/δ_H 3.66 (C-9), δ_C 70.30/δ_H 3.66 (C-2), δ_C 65.90/δ_H 3.69 (C-7), δ_C 75.02/δ_H 3.39 (C-8), δ_C 80.23/δ_H 3.68 (C-6), δ_C 81.03 (C-5), δ_C 173.26 (C-1, COO^-). Regarding structure 2, signals (ppm) of δ_C 22.84/δ_H 2.83 (C-3), δ_C 72.22/δ_H 4.72 (C-4), δ_C 72.34/δ_H 3.69 (C-9), δ_C 63.86/δ_H 3.78 (C-2), δ_C 64.95/δ_H 3.43 (C-7), δ_C 63.65/δ_H 3.68 (C-8), δ_C 72.27/δ_H 3.47 (C-6), δ_C 72.80/δ_H 3.66 (C-5), δ_C 173.09 (C-1, COO^-). Notably, regarding the carbonyl group, chemical shifts (ppm) of δ_C 173.09. Moreover, other signals might be ascribed to the structure of the tautomer. Anyway, the aforementioned tautomerization needs to be further proved, since some NMR signals were not discerned.

3.4. Volatile flavor compounds formed from the degradation of the thiazolidine derivatives

The Maillard reaction model system has always been the classic model reaction to study meat flavorings aroma compounds (Wei et al., 2020). Based on our previous studies, a stew meat-like flavor was produced from thiazolidine derivatives model system at pH 6.5, 140 °C, and 2 h (Du et al., 2023). A total of 109 flavor compounds were identified by GC-MS and GC-MS-O, as shown in Table 1, derived from the R 1, R 2, R 3, and R 4.

As shown in Table 1, R 1 system had detected 55 compounds, R 2 system had detected 61 compounds, R 3 system had detected 63 compounds, and R 4 system had detected 50 compounds. The four systems produced many lipids oxidative degradation compounds such as alcohols, ketones, aldehydes, and acids (shown in Table 1). This indicated that during heating, these thiazolidine derivatives were reversibly reacted to release the original reactants. Overall, the released aliphatic aldehydes undergo into degradation and polymerization process (shown in Fig. 4 a, b, c, d, e) (Du, et al., 2023; Shakoor et al., 2022). The degradation reaction during the heating of aliphatic aldehydes resulted in cracking the compound to form shorter aliphatic aldehydes. Whereas, in the polymerization process it forms aliphatic aldehydes with longer chains. Moreover, a study shown that enaldehydes also form dienaldehydes through oxidation or aldol condensation reactions (Wei et al., 2020).

R 1 system produced a very high amount of 2-heptylthiophene (meaty flavor). R 4 system produced a very high amount of 2-propylthiophene (sulfur flavor). The content of volatile compounds formed in the R 4 system, R 3 system, R 2 system, and R 1 system was in descending. The double bond content in thiazolidine derivatives contributes highly to reaction activity.

As shown in Table 1, alkyl sulfur-, oxygen-, or nitrogen-containing compounds (e.g., 2-pentylthiophene, 2-hexanoylfuran, and 2-butylpyridine) were found. This indicated that these reaction systems passed in the same way *via* these intermediates to form the aroma flavors (Mottram, 1998). Fig. 4 (d, e, f, g, h) also shown possible formation pathways of some identified compounds. Thiophenes were the most significant class of meat flavor compounds, and 2-propylthiophene, 2-pentylthiophene, and 2-heptylthiophene were the high-content compounds, where these flavor compounds were essential in meat food (Du et al., 2020; Sohail et al., 2022). As a study shown that 3-methyl-2-thiophenecarboxaldehyde, 2-hexylthiophene, 5-methyl-2-thiophenecarboxaldehyde, 2-pentylthiophene, and 2-thiophenecarboxaldehyde were detected in meat food (Sohail, et al., 2022). R 4 System had the most abundant thiophenes compared with other 3 systems. (*E,E*)-2,4-Octadienal, (*E,E*)-2,4-heptadienal, and (*E,E*)-2,4-decadienal reacting with H_2S could form the 2-butylthiophene, 2-propylthiophene, and 2-hexylthiophene, respectively.

The thiazoles with alkyl chains were generated in the 4 systems. This may be due to the degradation products of aliphatic aldehydes involved in the form pathway. With reported that the most commonly identified thiazoles were 4,5-dimethylthiazole and 2,4,5-trimethylthiazole (Du et al., 2020; Sohail et al., 2022). During heating, thermal degradation of the Strecker degradation of cysteine from thiazolidine derivatives induced by the aliphatic aldehyde degradation products can release H_2S and NH_3 (Shakoor et al., 2022; Zhao et al., 2019b). The high content of thiazole in R 2, R 3, and R4 may be due to the decarboxylation reaction of thiazolidine derivatives formed by the reaction of formaldehyde with cysteine, as shown in Fig. 4 (h).

The high level of 2-pentylfuran could be formed from nonanal and (*E*)-2-nonenal through alkene epoxidation and ring opening, cyclization, loss of water, and oxidization, as shown in Fig. 4 (f). Similarly, the identified 2-ethylfuran, 2-propylfuran, and 2-n-butylfuran from thiazolidine derivatives could result from cyclization of (*E*)-2-hexenal, (*E*)-2-heptenal, and (*E*)-2-octenal, in turn (Mottram, 1998). As reported in the literature, amino acids have catalytic function to catalyze the cyclization

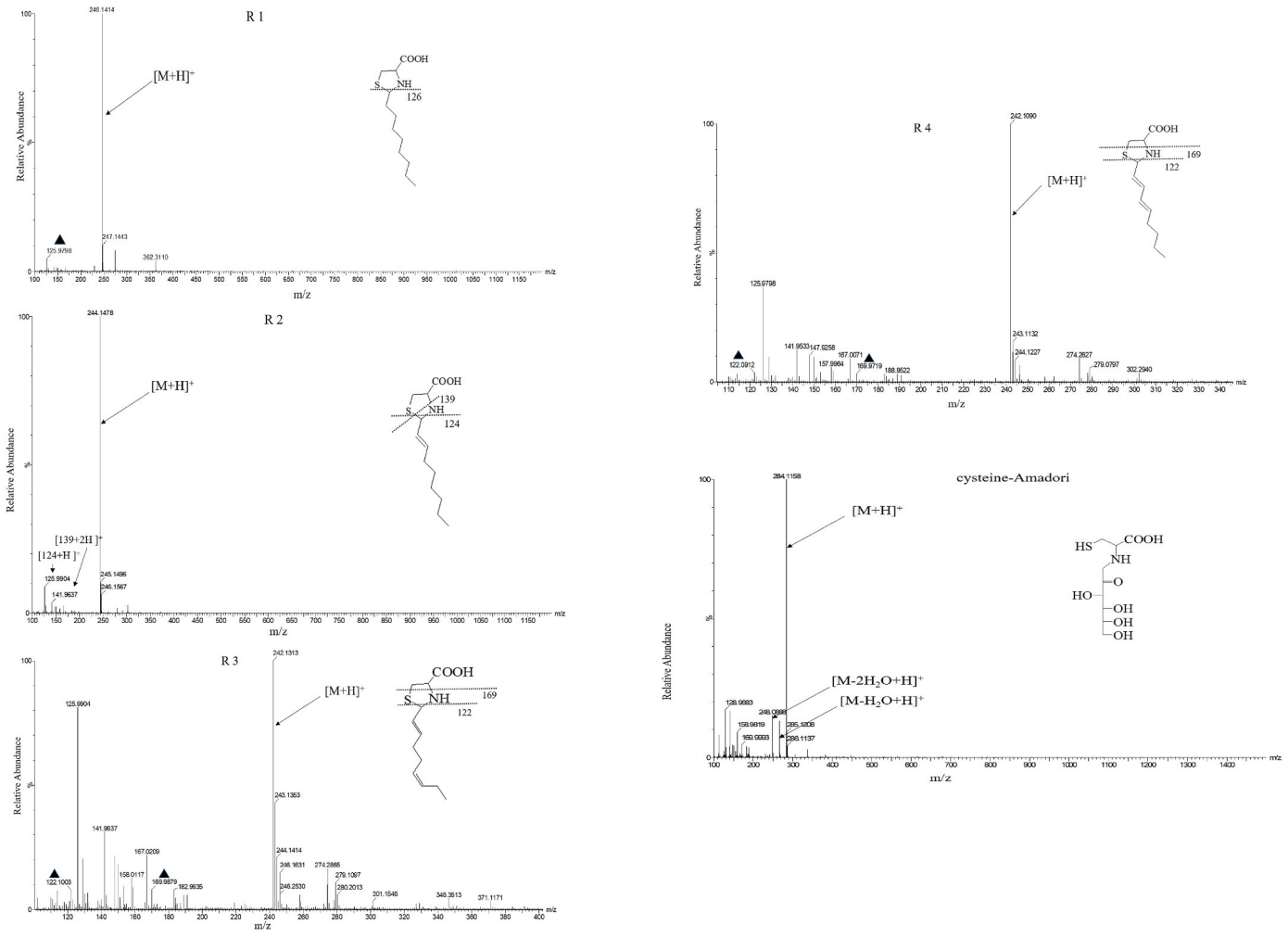

Fig. 3. Identified thiazolidine derivatives and Amadori compound by Q/TOF spectra.

of α,β-unsaturated aldehydes to form alkyl furans (Adams et al., 2011; Du et al., 2023; Xu et al., 2023).

2-Butylpyridine could be generated from aliphatic aldehydes in the same way as 2-pentylthiophene, with NH_3 involved instead of H_2S, as shown in Fig. 4 (d, e) (Mottram, 1998). The identified 1-hexanethiol in the R 2 system could be formed from the reaction of 1-hexanol and H_2S, while the reduction of hexanal could lead to the 1-hexanol (Wang et al., 2020).

4. Conclusions

In conclusion, in the processing of meat flavorings, concentrations of all the intermediates first rose and then fell with the extended reaction time, which was evidenced by their formation and degradation. The unsaturated aliphatic aldehydes contribute highly to reaction activity, mainly manifested in the inhibition of the cysteine-Amadori formation and acceleration of the thiazolidine derivatives formation. The effects of polyunsaturated on the initial Maillard reaction stage were similar. Cysteine as well were able to catalyze thiazolidine derivatives formation from the corresponding aliphatic aldehydes. Heating thiazolidine derivatives resulted in very complex flavor compound generation. Particularly, a route to form thiazole by the decarboxylation reaction of thiazolidine derivatives by cysteine reacting with formaldehyde was proposed. The work helps gain insight into the formation pathway of initial reaction intermediate compounds, and can also provide some guidance for processing of meat flavorings or meat foods.

Funding sources

The present work was supported by the Special National Key Research and Development Plan (2021YFD1600100), the Project of Science and Technology Department of Qinghai Province (2021-NK-A3), and the Shandong Province Key Research and Development Plan (2022CXGC010602).

Informed consent

Not applicable.

CRediT authorship contribution statement

Wenbin Du: Conceptualization, Data curation, Investigation, Methodology, Software, Supervision, Writing – original draft. **Yutang Wang:** Conceptualization, Formal analysis, Project administration, Writing – review & editing. **Qianli Ma:** Data curation, Supervision, Software. **Yang Li:** Supervision, Resources, Software. **Bo Wang:** Investigation, Formal analysis, Methodology. **Shuang Bai:** Data curation, Validation, Visualization. **Bei Fan:** Conceptualization, Funding acquisition, Project administration, Supervision, Resources, Writing – review & editing. **Fengzhong Wang:** Funding acquisition, Conceptualization, Formal analysis, Project administration, Writing – review & editing.

Table 1
Volatile aroma compounds derived from thiazolidine derivatives degradation.

[1]RI	Compounds	[2]Odor descriptors	[3]Quantity (μg/L)				[4]ID
			R 1	R 2	R 3	R 4	
	thiophenes						
1078	3-methylthiophene	sulfur	–	–	–	32.02 ± 0.76	RI/MS/O
1225	2-ethyl-5-methylthiophene	–	–	–	–	110.79 ± 2.00	RI/MS
1233	2-propylthiophene	sulfur	–	–	183.31 ± 2.86	853.78 ± 228.92	RI/MS/O/S
1241	2-ethenylthiophene	–	–	0.48 ± 0.01	122.82 ± 6.61	–	RI/MS
1253	3,4-dimethylthiophene	–	–	136.73 ± 27.77	–	53.97 ± 2.00	RI/MS/S
1340	2-butylthiophene	sulfur	32.40 ± 3.01	–	–	30.85 ± 2.00	RI/MS/O/S
1450	2-pentylthiophene	sulfur	–	630.92 ± 7.00	140.15 ± 11.11	–	RI/MS/O/S
1531	2-hexylthiophene	meaty	–	57.23 ± 7.24	–	–	RI/MS/O/S
1675	2-thiophenecarboxaldehyde	–	52.89 ± 5.82	–	95.57 ± 2.86	–	RI/MS/S
1652	2-heptylthiophene	meaty	1627.12 ± 66.72	24.63 ± 0.60	–	–	RI/MS/O/S
1785	5-methyl-2-thiophenecarboxaldehyde	sulfur	19.00 ± 5.68	–	–	476.37 ± 11.45	RI/MS/O/S
1817	1-(2-thienyl)-1-propanone	–	–	–	33.68 ± 2.20	–	RI/MS
1822	1-(2-thienyl)-1-butanone	–	–	–	73.27 ± 5.44	–	RI/MS
1837	thieno[3,2-b]thiophene	meaty	–	46.07 ± 0.78	–	–	RI/MS/O/S
1840	thieno[2,3-b]thiophene	meaty	65.95 ± 2.77	–	–	–	RI/MS/O/S
1942	2-ethyl-5-propylthiophene	–	–	–	438.71 ± 28.38	660.10 ± 57.23	RI/MS
1951	4-ethyl-2-propylthiophene	–	10.46 ± 0.29	–	–	–	RI/MS
2132	1-(2-thienyl)-1-heptanone	–	–	57.46 ± 1.91	–	–	RI/MS
2253	2-butyl-5-hexylthiophene	–	–	–	15.54 ± 1.33	–	RI/MS
	sum		1807.82	953.52	1103.05	2217.88	
	thiazoles						
	thiazole	–	–	136.74 ± 12.47	371.44 ± 15.49	79.95 ± 2.86	RI/MS/S
1301	4,5-dihydro-2-methylthiazole	–	–	94.90 ± 9.27	–	–	RI/MS
1304	2-ethylthiazole	roast	47.01 ± 5.82	139.45 ± 5.94	146.02 ± 7.91	634.83 ± 28.62	RI/MS/O/S
1363	4-methyl-5-ethylthiazole	–	–	–	1099.48 ± 15.35	180.00 ± 5.72	RI/MS
1374	4-propylthiazole	–	–	–	1248.40 ± 38.28	–	RI/MS
1376	2-propylthiazole	roast	–	15.29 ± 1.54	154.73 ± 12.90	48.00 ± 2.00	RI/MS/O/S
1411	5-ethyl-2-methylthiazole	–	–	240.81 ± 17.10	–	242.02 ± 5.72	RI/MS
1415	4-ethyl-5-methylthiazole	–	–	–	623.36 ± 39.14	–	RI/MS
1422	2-methyl-5-propylthiazole	–	–	27.93 ± 1.41	–	78.35 ± 11.45	RI/MS
1496	4,5-dimethyl-2-propylthiazole	–	–	33.48 ± 0.32	–	–	RI/MS
1523	2-butylbenzothiazole	–	–	–	75.27 ± 0.73	–	MS
	sum		47.01	688.6	3718.7	1263.15	
	furans						
955	2-ethylfuran	–	–	–		162.11 ± 2.78	RI/MS
1011	2-propylfuran	–	–	–	218.45 ± 1.15	–	RI/MS/S
1124	2-n-butylfuran	–	4.15 ± 0.82	–	83.15 ± 1.09	–	RI/MS
1152	2-butyltetrahydrofuran	–	600.32 ± 85.87		–	–	RI/MS
1231	2-pentylfuran	caramel	38.23 ± 5.81	435.36 ± 28.87	–	–	RI/MS/O/S
1416	(*E*)-2-(1-pentenyl)-furan	–	–	–	184.99 ± 11.27	–	RI/MS
1751	2-hexanoylfuran	–	–	5.17 ± 0.03	196.32 ± 11.02	–	RI/MS
1797	dihydro-5-propyl-2(3*H*)-furanone	caramel	414.44 ± 2.86	71.92 ± 1.40	–	–	RI/MS/O
1916	5-butyldihydro-2(3*H*)-furanone	–	211.76 ± 1.02	–	85.91 ± 7.21	–	RI/MS
2028	dihydro-5-pentyl-2(3*H*)-furanone	–	1141.07 ± 8.85	–	–	–	RI/MS
2132	3-hexyldihydro-2(3*H*)-furanone	caramel	–	–	262.90 ± 8.58	–	RI/MS
	sum		2409.97	512.45	1031.72	162.11	
	sulfides						
1149	1-hexanethiol	garlic	–	18.99 ± 0.23	–	–	RI/MS/O/S
1572	*anti*-3,5-dimethyl-1,2,4-trithiolane	–	3119.84 ± 142.43	10993.43 ± 790.31	–	11519.27 ± 94.43	RI/MS
1596	*syn*-3,5-dimethyl-1,2,4-trithiolane	–	–	–	–	3515.78 ± 1917.22	RI/MS
1730	1,2,3-trithiolane	–	–	708.69 ± 8.07	371.46 ± 0.34	1446.39 ± 34.34	RI/MS
1750	1,2,5-trithiepane	–	101.70 ± 5.72	–	99.51 ± 5.72	–	RI/MS
1815	4-methyl-1,2,3-trithiolane	–	35.86 ± 2.20	128.90 ± 0.60	–	992.60 ± 32.05	RI/MS
1918	1,3,5-trithiane	–	–	114.54 ± 4.01	–	–	RI/MS
2107	3-ethyl-5-methyl-1,2,4-trithiolane	–	–	501.44 ± 19.75	–	5231.98 ± 34.91	RI/MS
2159	2,4,6-trimethyl-1,3,5-trithiane	–	136.89 ± 67.86	1661.01 ± 219.90	–	1996.21 ± 50.36	RI/MS
	sum		3394.29	14127	470.97	24702.23	
	pyridines						
1214	2-methylpyridine	–	2.93 ± 0.73	–	–	30.08 ± 1.43	RI/MS/S
1282	3-ethylpyridine	–	–	–	–	726.57 ± 85.85	RI/MS
1311	2-ethylpyridine	–	–	–	–	73.19 ± 5.72	RI/MS
1375	3-propylpyridine	–	–	13.44 ± 3.05	80.54 ± 2.63	769.43 ± 57.23	RI/MS
1412	5-ethyl-2-methylpyridine	–	–	13.36 ± 1.59	–	297.63 ± 11.45	MS
1469	2-butylpyridine	–	129.28 ± 0.04	310.75 ± 18.72	1391.54 ± 51.12	144.81 ± 11.45	RI/MS
1572	2-pentylpyridine	burnt	–	–	559.34 ± 342.79	–	RI/MS/O/S
1758	2-hexylpyridine	–	–	49.91 ± 0.17	–	–	
	sum		132.21	387.46	2031.42	2041.71	
	aldehydes						
961	3-methylbutanal	–	–	12.80 ± 1.26	–	–	RI/MS
1058	2-butenal	–	72.88 ± 5.72	–	–	–	RI/MS/S
1097	hexanal	green	144.35 ± 5.72	463.41 ± 10.80	446.22 ± 15.27	–	RI/MS/O/S
1182	5-methylhexanal	–	122.21 ± 1.00	–	296.31 ± 1.54	–	RI/MS

(*continued on next page*)

Table 1 (*continued*)

[1]RI	Compounds	[2]Odor descriptors	[3]Quantity (μg/L)				[4]ID
			R 1	R 2	R 3	R 4	
1184	heptanal	green	43.22 ± 4.80	–	22.46 ± 4.39	318.64 ± 8.58	RI/MS/O/S
1297	octanal	green	–	–	124.32 ± 4.84	–	RI/MS/O/S
1322	(*E*)-2-heptenal	green	202.00 ± 2.86	–	1369.76 ± 13.70	–	RI/MS/O/S
1391	nonanal	fatty	–	–	5311.32 ± 210.40	–	RI/MS/O/S
1492	(*E,E*)-2,4-heptadienal	green	496.75 ± 5.72	–	–	–	RI/MS/O/S
1530	benzaldehyde	almond	24.97 ± 0.86	12.10 ± 0.47	619.25 ± 12.55	–	RI/MS/S
1544	(*E*)-2-nonenal	–	–	167.15 ± 21.27	206.28 ± 1.25	–	RI/MS
1642	2-methylbenzaldehyde	–	–	–	32.99 ± 1.98	–	RI/MS
1701	(*E,E*)-2,4-nonadienal	green	–	–	1528.30 ± 176.47	–	RI/MS/O/S
1715	(*E,Z*)-2,6-nonadienal	–	–	–	–	98.34 ± 11.45	RI/MS/S
1796	(*E,Z*)-2,4-decadienal	fatty	71.06 ± 5.72	–	–	–	RI/MS/O/S
1836	2-methylundecanal	–	572.98 ± 217.75	–	–	–	RI/MS
2209	2-pentyl-2-nonenal	–	–	–	347.31 ± 37.25	–	MS
2301	4-butylbenzaldehyde	–	–	–	1071.85 ± 116.41	–	MS
	sum		1750.42	655.46	11376.37	416.98	
	alcohols						
1125	1-butanol	–	–	–	64.65 ± 1.23	–	RI/MS
1158	1-penten-3-ol	mushroom	223.43 ± 5.72	–	–	281.00 ± 19.45	RI/MS
1252	1-pentanol	–	39.50 ± 21.07	177.43 ± 0.69	–	–	RI/MS/S
1361	1-hexanol	–	113.25 ± 1.60	350.70 ± 4.27	–	10.56 ± 0.29	RI/MS/S
1465	1-heptanol	–	642.48 ± 51.18	101.89 ± 3.11	–	–	RI/MS
1452	1-octen-3-ol	mushroom	–	8.24 ± 1.72	–	–	RI/MS
1540	2-octanol	soap	1021.90 ± 56.51	85.26 ± 2.56	–	–	RI/MS/O/S
1546	1-octanol	green	–	119.71 ± 19.67	240.00 ± 13.04	72.14 ± 8.58	RI/MS/O/S
1673	1-nonanol	soap	–	–	150.76 ± 24.20	–	RI/MS/O/S
1771	1-decanol	–	5730.43 ± 67.35	–	–	–	RI/MS
1775	5-decanol	–	–	344.36 ± 41.76	–	–	RI/MS
1982	1-dodecanol	–	–	28.28 ± 2.09	131.21 ± 13.61	–	RI/MS
	sum		7770.99	1215.87	586.62	363.7	
	ketones						
1097	2-hexanone	–	–	7.93 ± 0.47	–	415.97 ± 8.58	RI/MS
1287	2-octanone	sweet	1416.08 ± 97.31	2656.21 ± 121.56	20.73 ± 2.34	–	RI/MS/O/S
1317	2-octen-4-one	–	–	–	83.45 ± 2.68	383.33 ± 14.31	RI/MS
1357	3-nonanone	–	62.57 ± 2.86	3.20 ± 0.41	–	–	RI/MS
1390	2-nonanone	sweet	889.95 ± 8.71	858.05 ± 26.53	–	989.02 ± 114.46	RI/MS/O/S
1414	3-octen-2-one	–	–	–	1254.32 ± 135.57	410.10 ± 9.44	RI/MS/S
1492	5-decanone	–	–	–	418.54 ± 8.16	–	RI/MS
1599	2-undecanone	–	527.90 ± 6.84	–	–	–	RI/MS
	sum		2896.50	3525.39	1777.04	2198.42	
	acids						
1638	2-propenoic acid	–	60.31 ± 1.28	–	–	37.94 ± 0.29	RI/MS
1744	pentanoic acid	acid	–	–	23.69 ± 2.08	128.26 ± 5.72	RI/MS/O/S
1854	hexanoic acid	acid	269.83 ± 16.80	44.04 ± 1.17	–	–	RI/MS/O/S
1960	heptanoic acid	–	14.09 ± 1.24	177.04 ± 5.08	66.97 ± 14.34	–	RI/MS
2031	valproic Acid	–	–	6.81 ± 5.72	–	–	RI/MS
2066	octanoic acid	–	807.60 ± 17.16	123.44 ± 2.04	235.15 ± 24.95	123.79 ± 0.57	RI/MS/S
2097	2-methyloctanoic acid	–	846.77 ± 59.56	73.04 ± 1.74	–	–	MS
2174	nonanoic acid	–	949.62 ± 52.70	2161.75 ± 31.41	1784.96 ± 52.36	3139.34 ± 85.85	RI/MS/S
2181	n-decanoic acid	–	–	–	59.55 ± 2.57	241.96 ± 11.45	RI/MS
2192	8-methylnonanoic acid	–	109.53 ± 20.34	–	–	–	MS
2281	n-decanoic acid	–	–	44.06 ± 3.86	–	–	RI/MS/S
2325	dodecanoic acid	–	–	–	21.27 ± 1.09	–	MS
2331	(*E*)-2-dodecenoic acid	–	–	–	9.58 ± 0.29	–	RI/MS
2385	n-hexadecanoic acid	–	651.03 ± 8.60	–	–	–	MS
	sum		3708.78	2630.18	2201.17	3671.29	
	total		22917.99	24695.93	24297.06	37037.47	

[1]RI, retention indices determined using the DB-Wax capillary column (GC–MS/GC–MS-O analysis).
[2]The odor characteristics detected by GC-MS-O analysis of the thiazolidine derivatives degradation; "–", not detected.
[3]Quantity, the concentrations calculated from the peak area ratio of flavor compounds to the 1,2-dichlorobenzene; Different superscript letters in the same row indicated significant differences ($P < 0.05$); Note: "–", not detected.
[4]Identification methods.

Declaration of competing interest

No conflict of interest exits in the submission of this manuscript (entitled "The number and position of unsaturated bonds in aliphatic aldehydes affect meat flavorings system: Insights on initial Maillard reaction stage and meat flavor formation from thiazolidine derivatives"; authors: Wenbin Du, Yutang Wang, Qianli Ma, Yang Li, Bo Wang, Shuang Bai, Bei Fan*, Fengzhong Wang*), and manuscript is approved by all authors for publication. I would like to declare on behalf of my co-authors that the work described was original research that has not been published previously, and not under consideration for publication elsewhere. We declare that we do not have any commercial or associative interest that represents a conflict of interest in connection with the work submitted.

Data availability

No data was used for the research described in the article.

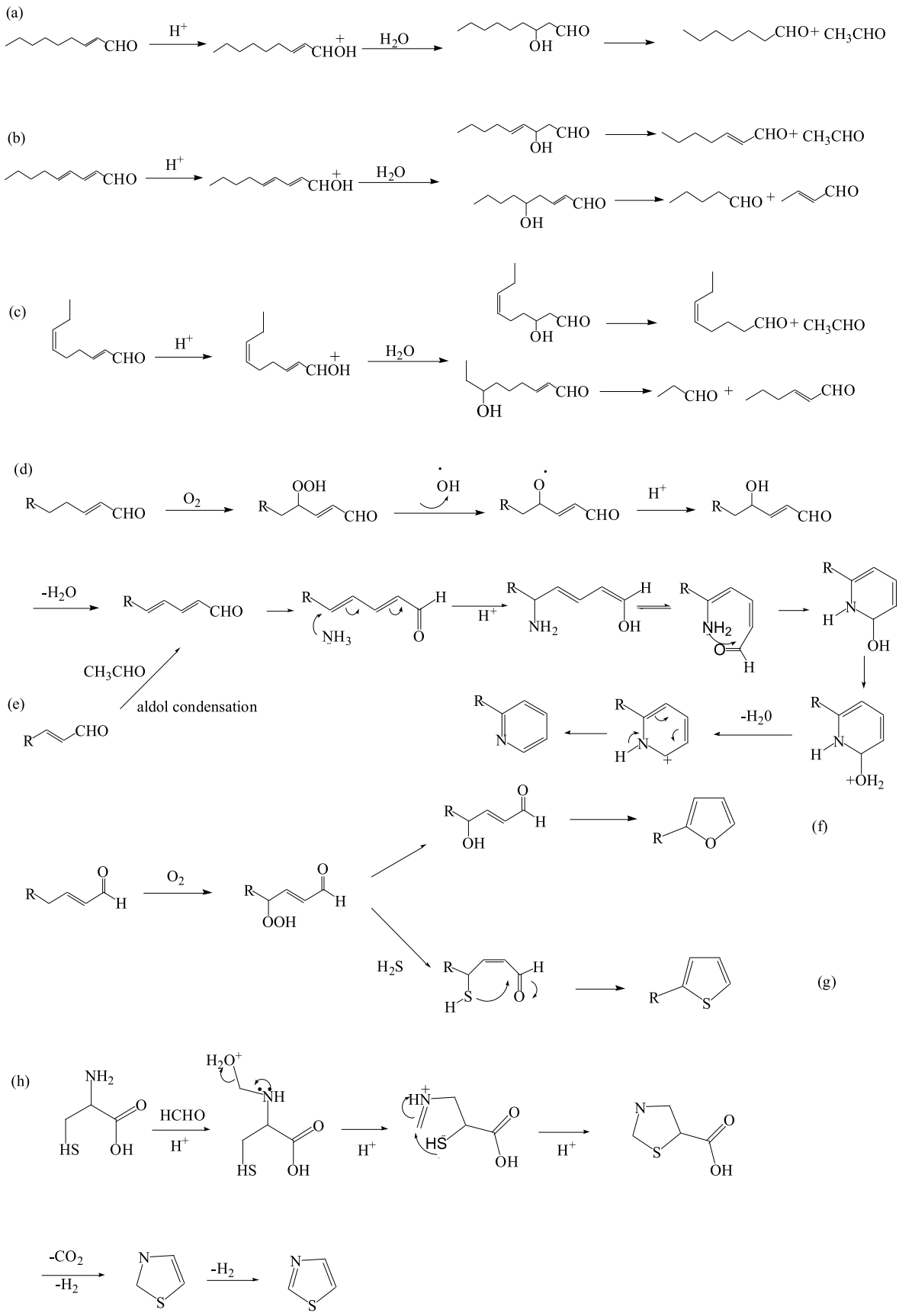

Fig. 4. (a) (b) (c) Formation of new aliphatic aldehydes from (*E*)-2-nonenal, (*E,E*)-2,4-nondienal and (*E,Z*)-2,6-nondienal *via* hydration and retro-aldol reaction. (d) (e)Formation of 2,4-dienal from 2-enal. (e) (f) (g) Proposed possible formation pathways for the alkyl thiophenes, furans, and pyridines. (h) Possible formation pathways for the thiazole.

Appendix A. Supplementary data

Supplementary data to this article can be found online at https://doi.org/10.1016/j.crfs.2024.100719.

References

Adams, A., Bouckaert, C., Van Lancker, F., De Meulenaer, B., De Kimpe, N., 2011. Amino acid catalysis of 2-alkylfuran formation from lipid oxidation-derived α,β-unsaturated aldehydes. J. Agric. Food Chem. 59 (20), 11058–11062. https://doi.org/10.1021/jf202448v.

Bi, S., Wang, A., Wang, Y., Xu, X., Luo, D., Shen, Q., Wu, J., 2019. Effect of cooking on aroma profiles of Chinese foxtail millet (*Setaria italica*) and correlation with sensory quality. Food Chem. 289, 680–692. https://doi.org/10.1016/j.foodchem.2019.03.108.

Cao, C., Xie, J., Hou, L., Zhao, J., Chen, F., Xiao, Q., Zhao, M., Fan, M., 2017. Effect of glycine on reaction of cysteine-xylose: Insights on initial Maillard stage intermediates to develop meat flavor. Food Res. Int. 99 (Pt 1), 444–453. https://doi.org/10.1016/j.foodres.2017.06.012.

Clark, A.C., Deed, R.C., 2018. The chemical reaction of glutathione and trans-2-hexenal in grape juice media to form wine aroma precursors: the impact of pH, temperature, and sulfur dioxide. J. Agric. Food Chem. 66 (5), 1214–1221. https://doi.org/10.1021/acs.jafc.7b04991.

Cui, H., Hayat, K., Jia, C., Duhoranimana, E., Huang, Q., Zhang, X., Ho, C.T., 2018. Synergistic effect of a thermal reaction and vacuum dehydration on improving xylose-phenylalanine conversion to *N*-(1-deoxy-d-xylulos-1-yl)-phenylalanine during an aqueous Maillard reaction. J. Agric. Food Chem. 66 (38), 10077–10085. https://doi.org/10.1021/acs.jafc.8b04448.

Du, W., Wang, Y., Yan, Q., Bai, S., Huang, Y., Li, L., Mu, Y., Shakoor, A., Fan, B., Wang, F., 2023. The number and position of unsaturated bonds in aliphatic aldehydes affect the cysteine-glucose Maillard reaction: formation mechanism and comparison of volatile compounds. Food Res. Int. 173 https://doi.org/10.1016/j.foodres.2023.113337.

Du, W., Zhao, M., Zhen, D., Tan, J., Wang, T., Xie, J., 2019. Key aroma compounds in Chinese fried food of youtiao. Flavour Fragrance J. 35 (1), 88–98. https://doi.org/10.1002/ffj.3539.

Du, W., Zhen, D., Wang, Y., Cheng, J., Xie, J., 2020. Characterization of the key odorants in grilled mutton shashlik with or without suet brushing during grilling. Flavour Fragrance J. 36 (1), 111–120. https://doi.org/10.1002/ffj.3621.

Fernandez, X., Duñach, E., Fellous, R., Lizzani-Cuvelier, L., Loiseau, M., Dompe, V., Cozzolino, F., George, G., Rochard, S., Schippa, C., 2001. Identification of thiazolidines in guava: stereochemical studies. Flavour Fragrance J. 16 (4), 274–280. https://doi.org/10.1002/ffj.996.

Hou, L., Xie, J., Zhao, J., Zhao, M., Fan, M., Xiao, Q., Liang, J., Chen, F., 2017. Roles of different initial Maillard intermediates and pathways in meat flavor formation for cysteine-xylose-glycine model reaction systems. Food Chem. 232, 135–144. https://doi.org/10.1002/ffj.996.

Li, X., Zhang, W., Zeng, X., Xi, Y., Li, Y., Hui, B., Li, J., 2023. Characterization of the major odor-active off-flavor compounds in normal and lipoxygenase-lacking soy protein isolates by sensory-directed flavor analysis. J. Agric. Food Chem. 71 (21), 8129–8139. https://doi.org/10.1021/acs.jafc.3c00793.

Mottram, D.S., 1998. Flavour formation in meat and meat products: a review. Food Chem. 62 (4), 415–425. https://doi.org/10.1016/S0308-8146(98)00076-4.

Pu, D., Shan, Y., Zhang, L., Sun, B., Zhang, Y., 2022. Identification and inhibition of the key off-oodorants in duck broth by means of the sensomics approach and binary odor mixture. J. Agric. Food Chem. 70 (41), 13367–13378, 0.1021/acs.jafc.2c02687.

Shakoor, A., Zhang, C., Xie, J., Yang, X., 2022. Maillard reaction chemistry in formation of critical intermediates and flavour compounds and their antioxidant properties. Food Chem. 393, 133416 https://doi.org/10.1016/j.foodchem.2022.133416.

Sohail, A., Al-Dalali, S., Wang, J., Xie, J., Shakoor, A., Asimi, S., Shah, H., Patil, P., 2022. Aroma compounds identified in cooked meat: a review. Food Res. Int. 157, 111385 https://doi.org/10.1016/j.foodres.2022.111385.

Wang, T., Zhen, D., Tan, J., Xie, J., Cheng, J., Zhao, J., 2020. Characterization of initial reaction intermediates in heated model systems of glucose, glutathione, and aliphatic aldehydes. Food Chem. 305, 125482 https://doi.org/10.1016/j.foodchem.2019.125482.

Wei, C.K., Ni, Z.J., Thakur, K., Liao, A.M., Huang, J.H., Wei, Z.J., 2020. Aromatic effects of immobilized enzymatic oxidation of chicken fat on flaxseed (*Linum usitatissimum L.*) derived Maillard reaction products. Food Chem. 306, 125560 https://doi.org/10.1016/j.foodchem.2019.125560.

Whitfield, F.B., 1992. Volatiles from interactions of Maillard reactions and lipids. Crit. Rev. Food Sci. Nutr. 31 (1–2), 1–58. https://doi.org/10.1080/10408399209527560.

Xu, Y., Bi, S., Xiong, C., Dai, Y., Zhou, Q., Liu, Y., 2023. Identification of aroma active compounds in walnut oil by monolithic material adsorption extraction of RSC18 combined with gas chromatography-olfactory-mass spectrometry. Food Chem. 402, 134303 https://doi.org/10.1016/j.foodchem.2022.134303.

Yang, Z., Xie, J., Zhang, L., Du, R., Cao, C., Wang, M., Acree, T., Sun, B., 2015. Aromatic effect of fat and oxidized fat on a meat-like model reaction system of cysteine and glucose. Flavour Fragrance J. 30 (4), 320–329. https://doi.org/10.1002/ffj.3248.

Yoshitake, J., Shibata, T., Shimayama, C., Uchida, K., 2019. 2-Alkenal modification of hemoglobin: Identification of a novel hemoglobin-specific alkanoic acid-histidine adduct. Redox Biol. 23, 101115 https://doi.org/10.1016/j.redox.2019.101115.

Yu, J., Zhang, S., Zhang, L., 2018. Evaluation of the extent of initial Maillard reaction during cooking some vegetables by direct measurement of the Amadori compounds. J. Sci. Food Agric. 98 (1), 190–197. https://doi.org/10.1002/jsfa.8455.

Zhao, J., Wang, T., Xie, J., Xiao, Q., Cheng, J., Chen, F., Wang, S., Sun, B., 2019a. Formation mechanism of aroma compounds in a glutathione-glucose reaction with fat or oxidized fat. Food Chem. 270, 436–444. https://doi.org/10.1016/j.foodchem.2018.07.106.

Zhao, J., Wang, T., Xie, J., Xiao, Q., Du, W., Wang, Y., Cheng, J., Wang, S., 2019b. Meat flavor generation from different composition patterns of initial Maillard stage intermediates formed in heated cysteine-xylose-glycine reaction systems. Food Chem. 274, 79–88. https://doi.org/10.1016/j.foodchem.2018.08.096.